42nd AIAA Aerospace Sciences Meeting
5-8 January 2004, Reno, Nevada
Paper: AIAA 2004-0337

QUANTUM SCATTERING STUDY OF RO-VIBRATIONAL EXCITATIONS IN $N+N_2$ COLLISIONS UNDER RE-ENTRY CONDITIONS

Dunyou Wang*, James R. Stallcop†, Christopher E. Dateo‡, David W. Schwenke§, and Winifred M. Huo¶
NASA Ames Research Center, MS T27B-1, Moffett Field, CA 94035-1000

Abstract

A three-dimensional time-dependent quantum dynamics approach using a recently developed *ab initio* potential energy surface is applied to study ro-vibrational excitation in $N+N_2$ exchange scattering for collision energies in the range 2.1– 3.2 eV. State-to-state integral exchange cross sections are examined to determine the distribution of excited rotational states of N_2. The results demonstrate that highly-excited rotational states are produced by exchange scattering and furthermore, that the maximum value of Δj increases rapidly with increasing collision energies. Integral exchange cross sections and exchange rate constants for excitation to the lower (v = 0–3) vibrational energy levels are presented as a function of the collision energy. Excited-vibrational-state distributions for temperatures at 2,000 K and 10,000 K are included.

Nomenclature

a_0	= Bohr radius, 5.291772×10^{-9}cm
a_i	= coefficient in Eq. (3)
D	= product vibrational distribution
E	= Total scattering energy
f	= subscript denoting final state
$\hbar$	= Plank constant
i	= subscript denoting initial state
j	= N_2 rotational quantum number
J	= total angular momentum
k	= reaction rate constant, cm^3/sec
P	= state-resolved reaction probability
r	= N–N separation distance, a_0
R	= distance between N and N_2 midpoint, a_0
t	= propagation time
T	= temperature, K
v	= N_2 vibrational quantum number
Δj	= change in value of j
κ	= Boltzmann constant
μ	= reduced mass
σ	= integral cross section, a_0^2
θ	= angle between r and R
Θ	= angle between r_a and r_b
Ω	= projection of J along z axis
Ψ	= time-dependent wave function
Ψ^+	= time-independent wave function

*Research Scientist, Eloret Corporation, Sunnyvale, CA; email: dwang@mail.arc.nasa.gov
†Physicist, Applications Branch, Nasa Advanced Supercomputing Division; email: James.R.Stallcop@nasa.gov
‡Senior Research Scientist, Eloret Corporation, Sunnyvale, CA; email: cdateo@mail.arc.nasa.gov
§Chemist, Applications Branch, Nasa Advanced Supercomputing Division; email: David.W.Schwenke@nasa.gov
¶Group Lead, Applications Branch, NASA Advanced Supercomputing Division; email: Winifred.M.Huo@nasa.gov

Introduction

In a recent shock tube experiment using nitrogen gas, Fujita et al.[1] measured the rotational and vibrational temperatures using the N_2 2nd postive and N_2^+ first negative bands and found significant nonequilibrium between the measured rotational and translational temperatures. This result is in apparent violation of the two-temperature model of Park[2], one of the standard models widely used in the analysis of nonequilibrium aerothermodynamics. The observed deviation led to two studies of nitrogen rotational excitations behind a strong shock wave. Fujita and Abe[3] carried out quasi-classical trajectory (QCT) calculations of state-to-state rotational

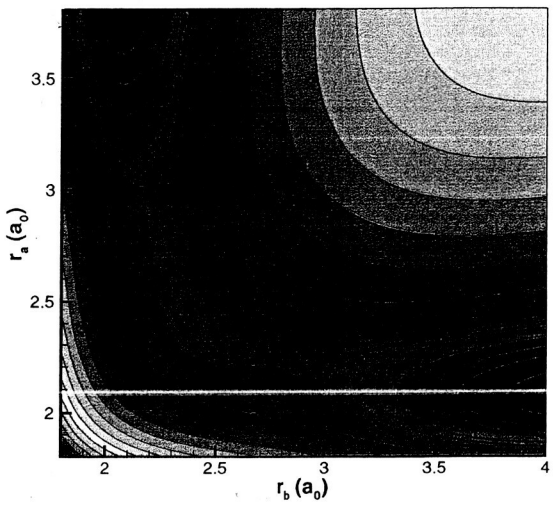

FIG. 1: Contour plot of the WSHDSP *ab initio* PES of the N+N_2 interaction region in terms of the two N–N bond lengths r_a and r_b; Θ is fixed at 120°.

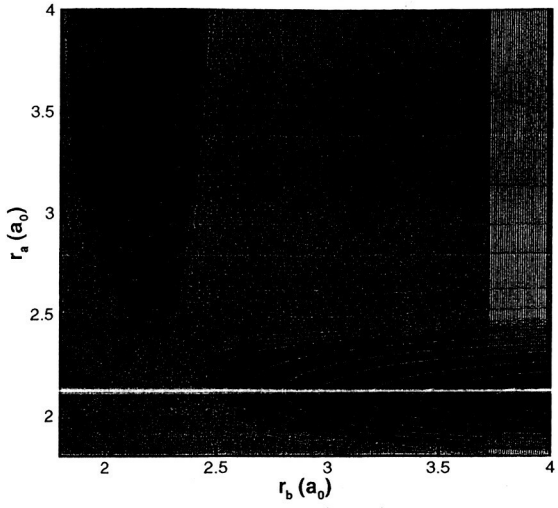

FIG. 2: Contour plot of the LEPS PES for the N+N_2 interaction region of Fig 1 in terms of the two N–N bond lengths r_a and r_b; Θ is fixed at 180°.

excitation rates in N_2+N_2 collisions using the empirical N_2–N_2 intermolecular potential energy of Billing and Fisher[4]. Their calculation covered transitions with very large (well over 100) Δj, which is the change in the N_2 rotational state quantum number j .Their QCT rate differed significantly from the empirical Rahn-Palmer[5] rate formula above 3000 K. Simultaneously, Park[6] extended the Rahn-Palmer formula to large Δj and high temperature. His results appeared to agree reasonably well with the shock tube data of Sharma and Gillespie[7] and Ref. 1.

Both approaches, the calculation of Ref. 3 and the Rahn-Palmer extension of Ref. 6 have substantial shortcomings that make their predictions unreliable. Stallcop and Partridge[8] have constructed a potential energy surface (PES) for N_2–N_2 interactions that is based on accurate short-range *ab initio* results from high-level quantum structure calculations; the van der Waals interaction and the long-range behavior of this PES have been validated[9] by very accurate results from a bond-function calculation. Knowing the anisotropy of the actual N_2–N_2 interaction energy assists our assesment of the reliability of the two approches.

The N_2–N_2 interaction energy used in calculation of Ref. 3 was developed in Ref. 4 to study V-V and V-T energy transfer rates. Rotational motion was not quantized in Ref. 4, but was considered to be part of the translational motion. The angular dependence of the repulsive interaction energy was represented by the factors: $cosh(\epsilon_i)$ with $\epsilon_i = 0.5\alpha r_i cos\gamma_i$, where r_i is the N-N separation distance of the ith N_2 molecule and γ_i the angle between r_i and R, which is the separation distance of the center of masses of the two N_2 molecules. Also, α is a parameter that specifies the the range of the repulsive potential energy. The use of the $cosh(\epsilon_i)$ factors is unusual. Because the repulsive interaction energy of Ref. 4 does not fully reflect the the symmetry of the N_2–N_2 interaction, it can lead to very high Δj transitions that are physically unrealistic. It has been shown that the angular variation of the repulsive potential energy of the accurate interaction energy can be represented by a relatively simple form[8], but it is very different from that of Ref. 4. Because rotational motion was not explicitly accounted for in the calculation of Billing and Fisher, the above factors did not create readily-discernable problems in their results[4]. On the other hand, rotational motion was quantized in the study of Ref. 3. The $cosh(\epsilon_i)$ factors were the source of very large Δj transitions, which would not have been found if a more realistic N_2–N_2 interaction energy had been used.

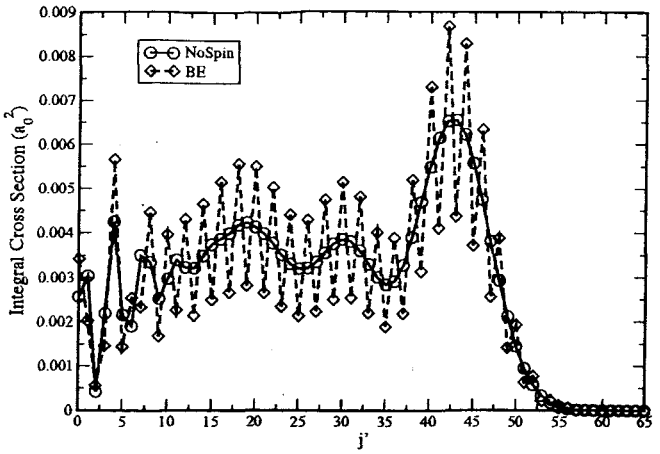

FIG. 3: State-to-state integral cross sections for exchange scattering, with rotational state excitation, $N + N_2(v = 0, j = 0) \rightarrow N_2(v' = 0, j') + N$, vs. j for total scattering energy at 2.5 eV. The symbols ○ and ◇ represent the results obtained by neglecting nuclear spin and using Bose-Einstein statistics, respectively. The discrete data points are joined by straight-line curves for clarity.

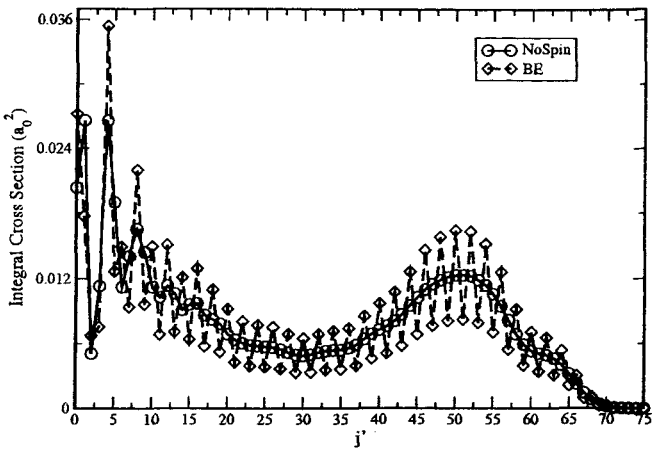

FIG. 4: Similar to Fig. 3 except that the total scattering energy is at 3.0 eV.

The extension of the Rahn-Palmer formula used in Ref. 6 to predict rotational excitation at large Δj and high temperatures probably also produces unphysical results. The Rahn-Palmer formula is fitted to experimental data only up to 3000 K; the largest observed Δj was 14. Extrapolation to very large Δj (such as more than 100) is beyond the range of validity of this formula. Based on the actual N_2–N_2 interaction energy described above, we conclude that such highly anisotropic interaction is probably unphysical.

While it is likely that the large Δj transitions indicated in the shock tube data of Ref. 1 do not come from N_2–N_2 collisions, the N–N_2 exchange mechanism can lead to such transitions at the high temperature regime of the experiment. Exchange reactions are important phenomema for real-gas analysis. For example, like ion–atom diffusion processes are dominated by resonance charge exchange.

In the atom exchange reaction

$$N + N_2(v, j) \rightarrow N_2(v', j') + N, \qquad (1)$$

the N-N bond in the original N_2 molecule is broken and a new N-N bond is formed. Due to the nature of the N+N_2 interaction energy as described below, the new N_2 molecule may have a highly-excited rotational state (compared to the rotational state of the original molecule).

Among more recent model calculations, Esposito et al.[10,11] have calculated N+N_2 scattering using a quasi-classical method and a semiempirical London-Eyring-Polany-Sato (LEPS) interaction energy. All but one of parameters of the LEPS model have been obtained[12] from the potential energy well of a ground-state N_2 molecule or an extrapolation using a Morse-potential-energy fit; the remaining parameter specifies the height of a transition state barrier and has been estimated from the results of limited measurement.

A theoretical determination of exchange scattering must be based on a quantum mechanical description. For example, the N–N^+ resonance charge exchange[13] would be underestimated by almost an order of magnitude using classical mechanics. The first *ab initio* potential energy surface for the N_3 system (WSHDSP PES) that includes variation in the interatomic separation distances of the N_2 molecules and the first quantum dynamics study of the cumulative reaction probabilities and chemical reaction rates of the N+N_2 exchange reaction have recently been reported by our group[14].

The WSHDSP[14] PES for N_3 is constructed from the results of high-level quantum structure calculations. These calcuations are primarily based on the same methods that were used to determine the *ab initio* data for the construction of the very accurate N+N_2 rigid-rotor PES of Stallcop et al.[15]; long-range dispersion force data and nearly 4000 *ab initio* data points, are applied to construct our present N_3 PES. The reaction region of the PES con-

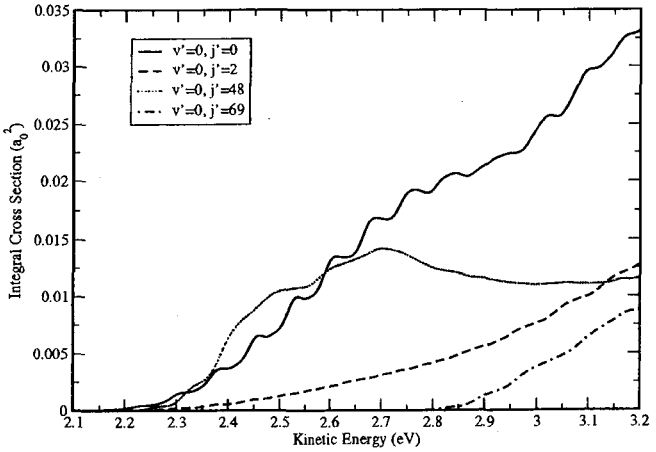

FIG. 5: State to state integral cross sections for exchange scattering with with rotational state excitation, N + $N_2(v = 0, j = 0) \rightarrow N_2(v' = 0, j') + N$, as a function of the kinetic energy.

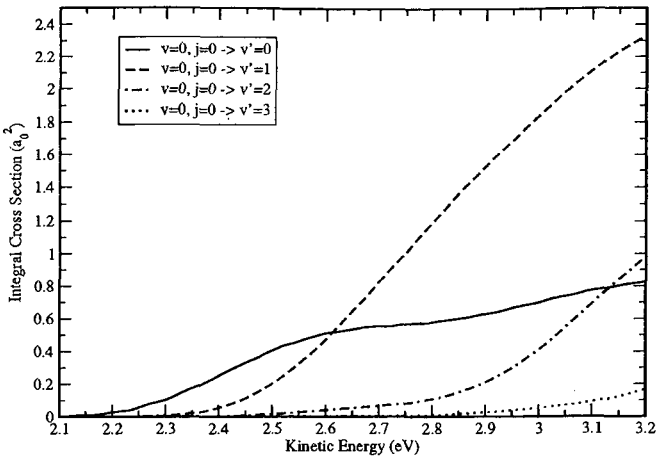

FIG. 6: Integral cross sections for exchange scattering with N + $N_2(v = 0, j = 0) \rightarrow N_2(v') + N$ as a function of kinetic energy; $v' = 0$–3.

tains two transition state barriers, which are equivalent with respect to interchange of two nitrogen atoms, that are separated by a shallow well. The *ab initio* PES[14] and the results from a semiempirical model[12] are represented by contour plots in Figs. 1 and 2, respectively. Note the large difference in the behaviors of the actual and semiempirical PES in the reaction region.

The reaction geometries of our PES is specified by: $r_a(r_b) = 2.23$ bohr, $r_b(r_a) = 2.80$ bohr, and $\Theta = 119^o$ for the transition states and $r_a = r_b = 2.40$ bohr and $\Theta = 120^o$ for the well minimum; r_a and r_b are the two N-N bond lenths and Θ is the angle between r_a and r_b. The transition state is located at 2.05 eV above the energy of the N+N_2 asymptote, and the well minimum is at 1.90 eV. The shallow well of the double hump in the reaction region has been dubbed[16,17] "Eyring's lake" in studies of other interactions; in the discussion below, we use the term 'Lake Eyring' to identify certain features associated with reaction region of the N_3 PES.

In addition to the attributes noted above, a quantum mechanical description of the scattering can account for inelastic scattering reasonances and effects due to nuclear spin symmetry. We have found[18,19] that N+N_2 exchange scattering exhibits profuse Feshbach resonance structures and furthermore, that these resonances arise from N_3 vibrational energy levels lying above the shallow well of the transition-state region of the PES.

Theoretical Method

The 3D quantum dynamics of the state-to-state reaction calculation is carried out using a time-dependent wave packet method[20,21]; this method is summarized briefly below. The split-operator[22] propagation scheme is used for wave packet propagation. Also, a two-stage propagation approach is employed to calculate the state-resolved reaction probability. First, an initial wave packet for a given total angular momentum J, located in the reactant asymptotic region and covering the translational energy from 2.0 eV to 3.2 eV, is propagated in the reactant Jacobi coordinates on the *ab initio* PES, until it enters into the transition state region after about 2000 atomic units of time. At this stage, its position representation is transformed from the reactant into the product Jacobi coordinates and the propagation is continued.

After the wave packet enters into the product asymptotic region, the energy-dependent state-resolved reaction probability $P_{fi}(E)$ for energy E is obtained from the flux passing through a dividing surface in the product asymptotic region

$$P_{fi}(E) = \frac{\hbar}{\mu} Im[\Psi_{fi}^{+*}(E, R') \frac{\partial}{\partial R'} \Psi_{fi}^{+}(E, R')]|_{R'=R'_f}, \quad (2)$$

where μ is the reduced mass of the system. The quantities i and f represent the set of quantum numbers v, j, J, Ω and v', j', J, Ω' for the initial and final states, respectively. Also, R is the translation Jacobi coordinate that connects an N atom to the center mass of the N_2

molecule; unprimed or primed indicates that the coordinate system is located in the reactant or product channel, respectively. The quantity R'_f is the position of the dividing surface in the product asymptotic region where the reaction is complete and the flux is invariant with respect to moving R'_f further away from the interaction region. The time-independent scattering wavefunction $\Psi^+_{fi}(E, R')$ is obtained by performing a Fourier transform of the time-dependent wave equation $\Psi_i(t)$; *i.e.*,

$$\Psi^+_{fi}(E, R') = \frac{1}{a_i(E)} \int_{-\infty}^{+\infty} e^{i\frac{E}{\hbar}t} < f, R'|\Psi_i(t) > dt. \quad (3)$$

where the coefficient $a_i(E)$ is given by the overlap[23] between the initial wave packet $\Psi_i(0)$ and the normalized asymptotic scattering function.

Since a two-stage propagation scheme is employed to calculate the state-to-state reaction probability, there are two sets of basis functions for this calculation. One set is for the reactant channel, with 220 sine functions to represent R from 2.3 a_0 to 10.4 a_0, 100 vibrational eigenfunctions of N_2 to cover the vibrational coordinate (N–N separation distance) r from 1.3 a_0 to 5.5 a_0, and 70 even Legendre functions (j_{max}=140) or 70 odd Legendre functions (j_{max}=139) to cover θ, which is defined to be the angle between R and r. The other set is for the product channel, where 320 sine functions are used for R' in the range from 0.1 a_0 to 14.0 a_0, 220 vibrational functions for expansions of r' from 0.1 a_0 to 12.0 a_0, and 150 Legendre functions for θ'. As described above, the wave packet first propagates in the reactant channel and then it is transformed into the product-channel coordinates. Finally, it is propagated for 8000 atomic units of time in the product channel. The state resolved flux is calculated at R'_f=10.0 a_0. The whole calculation has been carried out using 32 CPU on a SGI Origin 3000 system. About 40,000 CPU hours were required for the state-resolved calculations described here.

When nuclear spin is ignored (no-spin), the integral cross section can be obtained by summing over all partial waves J

$$\sigma_{v'j'\leftarrow vj} = \frac{\pi}{k_i^2(2j+1)} \sum_{J=0} (2J+1) P^J_{v'j'\leftarrow vj}(E). \quad (4)$$

where $P^J_{v'j'\leftarrow vj}(E)$ is obtained from the P_{fi} of Eq. (1) by summing over Ω and Ω'. The quantity k_i in Eq. (4) comes from the initial-state wave vector.

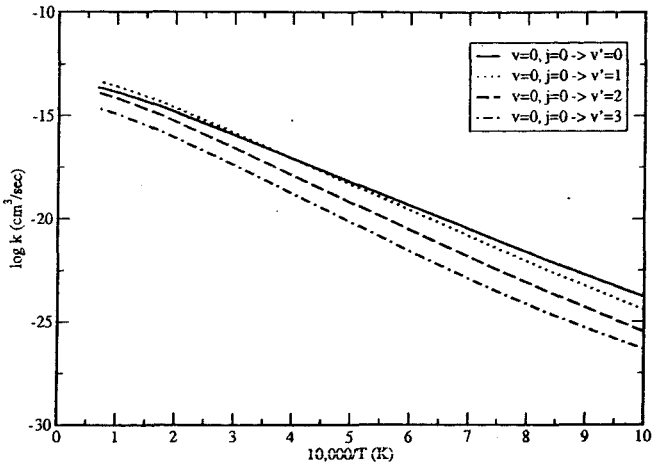

FIG. 7: Exchange rate constant for N + $N_2(v = 0, j = 0) \rightarrow N_2(v')$ + N; T is in K, k is in cm^3/sec, and $v' = 0$–3.

Since the nitrogen atoms have identical nuclei (99.7% of nitrogen consists of the ^{14}N isotope), the N+N_2 cross section $\bar{\sigma}$ is obtained from sums and averages over the nuclear spin states. The nuclear spin of nitrogen atom is equal to 1; hence, the N+N_2 scattering obeys Bose-Einstein (BE) statistics. The cross sections with the appropriate nuclear spin factors become

$$\bar{\sigma}_{v'j'\leftarrow vj} = \begin{cases} \frac{4}{3}\sigma_{v'j'\leftarrow vj} & \text{if } j' \text{ is even,} \\ \frac{2}{3}\sigma_{v'j'\leftarrow vj} & \text{if } j' \text{ is odd.} \end{cases} \quad (5)$$

Results and Discussion

Rotational Excitation

The determination of the state-to-state integral cross section requires summing over 96 partial waves (*i.e.*, from $J = 0$ to $J_{max} = 95$) to obtain convergence for kinetic energies in the range from 2.0 eV to 3.2 eV. State-to-state integral cross sections for scattering energies at 2.5 eV and 3.0 eV are given in Figs. 3 and 4, respectively, to illustrate the distribution of rotational state excitation. Note that we plot both results, one with nuclear spin based on Bose-Einstein statistics and the other without spin. Since the nuclear spin factors of Eq. (5) introduce rapid oscillations in the cross sections, resonance features in the cross sections are more easily recognizable using the data without nuclear spin. In Fig. 3, strong oscillations occur at low j' and at the three major reactive resonances centered at j' = 19, 30, and 43. There is no

significant excitation to rotational states with j' larger than 57. Comparison of Fig. 3 with the similar results shown in Fig. 10 of Ref. 19 for a scattering energy at 2.4 eV shows that the excited rotational distribution is quite sensitive the scattering energy. Fig. 4 shows that higher (up to $j' = 70$) rotational states of N_2 are excited at a higher scattering energy. Furthermore, the integral cross sections are larger at higher scattering energies; strong oscillations are also found at low j' and have a variation similar to that shown in the figures discussed above.

Figure 5 shows $\sigma_{v'j'\leftarrow vj}$ for scattering from a ($v = 0, j = 0$) initial ro-vibrational state to various final ro-vibrational states. The curves of $\sigma_{0j'\leftarrow 00}$ for low-lying final ro-vibrational states, such as the ($v' = 0, j' = 0$) and ($v' = 0, j' = 2$) states, have an oscillating behavior arising from reactive resonances. As described above, these resonances have been shown[18,19] to be caused by metastable states of the 'Lake Eyring' region of the PES. Here they appear, primarily, as 'bumps' in the state-to-state integral cross sections. However, for higher final ro-vibrational states, *e.g.*, ($v' = 0, j' = 48$) and ($v' = 0, j' = 69$) states, the resonances are washed out by the sum over the partial waves. Fig. 5 also shows that the integral cross section for $j = 0 \rightarrow j' = 2$ has a much smaller magnitude than that for $j = 0 \rightarrow j' = 48$ at lower kinetic energies. The variation of the large cross sections for producing high j', such as $j = 0 \rightarrow j' = 48$, with kinetic energy verifies that the N+N_2 exchange reaction is quite efficient for producing high rotational levels of N_2 molecules.

The above results for rotational excitation indicate that the exchange reaction of N+N_2 collisons provides a mechanism to pump N_2 molecules with low rotational states into N_2 molecules with higher rotational states. Because this exchange reaction has a propensity for producing highly excited rotational states, it provides a route that may lead to nonequilibrium rotational temperature behind a strong shock.

Vibrational Excitation

The integral cross section for v' excitation from a ($v = 0, j = 0$) initial ro-vibrational state is obtained by summing over all the final rotational states ; *i.e.*,

$$\sigma^*_{v'\leftarrow 00} = \sum_{j'} \sigma_{v'j'\leftarrow 00}. \qquad (6)$$

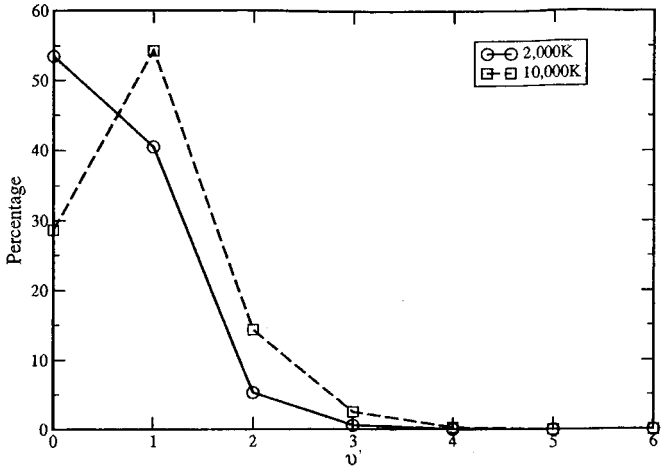

FIG. 8: The product vibrational distribution for N + N_2($v = 0, j = 0$) $\rightarrow$ $N_2(v')$ + N vs. v'. The discrete data for each value of T (at 2000 and 10,000 K) are joined by straight-line curves for clarity.

The values of $\sigma^*_{v'\leftarrow 00}$ are shown in Fig. 6 for $v' = 0$–3. This figure shows that significant vibrational excitation of N_2 is produced by exhange reactions at higher kinetic energies. In particular, this figure shows that at lower kinetic energies, the largest integral cross section is found for $v' = 0$. However, at higher energies the order is different; for example, at 3.2 eV the order is: $\sigma^*_{1\leftarrow 00} > \sigma^*_{2\leftarrow 00} > \sigma^*_{0\leftarrow 00} > \sigma^*_{3\leftarrow 00}$. In other words, at this energy, the vibrational products are larger at higher ($v' = 2$ and $v' = 1$) vibrational levels than at the lower ($v' = 0$) vibrational level. Furthermore, the $v' = 3$ vibrational state does not have a major role in the final state distributions at this energy.

Rate Constants

The reaction rate constant $k_{v'\leftarrow 00}(T)$, for exchange scattering from the ($v = 0, j = 0$) initial ro-vibrational state to the (v', j') final ro-vibrational states for all j', is obtained from

$$k_{v'\leftarrow 00}(T) = \sqrt{\frac{8}{\kappa^3 T^3 \pi \mu}} \int dE exp(-E/\kappa T) E \sigma^*_{v'\leftarrow 00}(E). \qquad (7)$$

We present $k_{v'\leftarrow 00}(T)$ for $v' = 0$–3 in Fig. 7. Note that the rates can be represented fairly well by straight lines except at high T where there is a small fall-off; the integration of Eq. (7) has been truncated at the the highest energy of this study.

The product vibrational distributions are calculated

from the equation

$$D_{v'\leftarrow 00}(T) = k_{v'\leftarrow 00}(T)/\sum_{v''} k_{v''\leftarrow 00}(T). \qquad (8)$$

Figure 8 shows $D_{v'\leftarrow 00}(T)$ for T = 2,000 K and 10,000 K. Note that the distribution of the final vibrational states of N_2 is more concentrated at low v'. As T increases, the peak of the distribution moves to a higher-lying vibrational state as expected.

Concluding Remarks

Our calculations demonstrate that the N+N_2 exchange reaction could result in a rotational distribution that is very much in nonequilibrium. This was not predicted by a previous QCT study[10,11] of N+N_2 collisions because the LEPS interaction energy[12], which was used for their study, does not have the 'Lake Eyring' feature. Furthermore, the resonance structures in the reaction probability are quantal features that are not amenable to classical treatment.

One might disregard like-atom exchange from atom-molecule collisions since there is no change in the population density of the constituents of the gas; the above study, however, demonstrates that these reactions could significantly change the energy distribution among the constituents. Furthermore, we point out that the above approach, construction of a PES from *ab initio* data and subsequent quantum-dynamical calculation of the atom-molecule reactions, can also be applied to determine the exchange reaction for unlike atoms, such as

$$O + N_2 \rightarrow NO + N. \qquad (9)$$

The use of model interaction energies in scattering calculations may reproduce the results of certain experiments, but we emphasize that, in general, the results of these calculations do not provide reliable thermodynamic properties, especially at high temperatures.

Direct N+N_2 inelastic collisions, which do not involve any bond breakage and formation, will lead to low Δj transitions until the kinetic energy is at or above the onset of exchange reaction. In this region, the resonances that play such an important role in exchange collisions also affect inelastic collisions and large Δj transitions are expected from these inelastic collisions, as well as that found for the exhange reactions.

We plan to study ro-vibrational excitations in N+N_2 inelastic collsions. The inelastic results from direct scattering will then be incorporated with the present results for N+N_2 exchange collisions. The data will be used to similate the shock tube experiments of Refs. 1 and 7. Rotational and vibrational temperatures under high-speed entry conditions will also be studied.

[1] Fujita, K., Sato, S., Abe, T., and Ebinuma, Y., "Experimental Investigation of Air Radiation from behind a Strong Shock Wave," *Journal of Thermophysics and Heat Transfer*, Vol. 16, No. 1, 2002, pp. 77-82.

[2] Park, C., "Review of Chmical-Kinetic Problems of Future NASA Missions I: Earth Entries," *Journal of Thermophysics and Heat Transfer*, Vol. 7, No. 3, 1993, pp. 385-398.

[3] Fujita, K., and Abe, T., "State-to-State Nonequilibrium Rotational Kinetics of Nitrogen Behind a Strong Shock Wave," AIAA paper 2002-3218, 8th AIAA/ASME Joint Thermophysics and Heat Transfer Conference, June 2002.

[4] Billing, G. D., and Fisher, E. R., "VV and VT Rate Coefficients in N_2 by a Quantum-Classical Model", *Chemical Physics*, Vol. 43, No. 3, 1979, pp. 395-401.

[5] Rahn, L. A., and Palmer, R. E., "Studies of Nitrogen Self-Broadening at High Temperature with Inverse Raman Spectroscopy," *Journal of the Optical Society of America B*, Vol. 3, No. 9, 1986, pp. 1164-1169.

[6] Park, C., "Rotational Relaxation of N_2 Behind a Strong shock wave", AIAA paper 2002-3218, 8th AIAA/ASME Joint Thermophysics and Heat Transfer Conference, June 2002.

[7] Sharma, S. P., and Gillespie, W., "Nonequilibrium and Equilibrium Shock Front Radiation Measurement," *Journal of Thermophysics and Heat Transfer*, Vol. 5, No.3, 1991, pp. 257-265.

[8] Stallcop, J. R., and Partridge, H., "The N_2–N_2 Potential Energy Surface," *Chemical Physics Letters*, Vol. 281, No.2, 1997, pp. 212-220.

[9] Stallcop, J. R., Partridge, H., and Levin., E., "Effective Potential Energies and Transport Cross Sections for Interactions of Hydrogen and Nitrogen," *Physical Review A*, Vol. 62, No. 6, 2000, pp. 062709(1-15).

[10] Esposito, F., and Capitelli, M., "Quasiclassical Molecular Dynamic Calculations of Vibrationally and Rotationally State Selected Dissociation Cross Sections: N+N_2 → 3N," *Chemical Physics Letters*, Vol. 302, No. 1, 1999, pp. 49-54.

[11] Esposito, F., Capitelli, M., and Gorse, C., "Quasi-Classical Dynamics and Vibrational Kinetics of N+$N_2(v)$ System," *Chemical Physics*, Vol. 257, No. 2, 2000, pp. 193-202.

[12] Laganà, A., Garcia, E., and Ciccarelli, L., "Deactivation of Vibrationally Excited Nitrogen Molecules by Collision

with Nitrogen," *Journal of Physical Chemistry*, Vol. 91, No. 3, 1987, pp. 312-314.

[13] Stallcop, J. R., Partridge, H., and Levin, E., "Resonance Charge Transfer, Transport Cross Sections, and Collision Integrals for $N^+(^3P)$–$N(^4S^0)$ and $O^+(^4S^0)$–$O(^3P)$ Interactions," *Journal of Chemical Physics*, Vol. 95, No. 9, 1991, pp. 6429-6439.

[14] Wang, D. Y., Stallcop , J. R., Huo, W. M., C. E. Dateo, Schwenke, D. W., and Partridge, H., "Quantal Study of the Exchange Reaction for $N+N_2$ Using an *Ab Initio* Potential Energy Surface," *Journal of Chemical Physics*, Vol. 118, No. 5, 2003, pp. 2186-2189.

[15] Stallcop, J. R., Partridge, H., and Levin, E., "Effective Potential Energies and Transport Cross Sections for Atom–Molecule Interactions of Nitrogen and Oxygen," *Physical Review A*, Vol. 64, No.4, 2001, pp. 042722(1-12).

[16] Eyring, H., Walter, J., and Kimball, G. E., *Quantum Chemistry*, J. Wiley and Sons, New York, 1944.

[17] Mladenović, M., Botschwina, P., Sebald, P., and Carter, S., "A Theoretical Study of the Acetylide Anion, HCC^-," *Theoretical Chemistry Accounts*, Vol. 100, No. 1, 1998, pp. 134-146,

[18] Wang, D. Y., Huo, W. M., Dateo, C. E., Schwenke, D. W., and Stallcop, J. R., "Reactive Resonances in the $N+N_2$ Exchange Reaction," *Chemical Physics Letters*, Vol. 379, No. 1, 2003, pp. 132-138.

[19] Wang, D. Y., Huo, W. M., Dateo, C. E., Schwenke, D. W., and Stallcop, J. R., "Quantum Study of the $N+N_2$ Exchange Reaction: State-to-State Reaction Probabilites, Initial-State Selected Probalities, Feshbach Resonance, and Product Distributions," Accepted for publication by *Journal of Chemical Physics*, 2003.

[20] Zhang, D. H., and Zhang, J. Z, H., "Quantum Reactive Scattering with a Deep Well: Time-Dependent Calculation for $H+O_2$ Reaction and Characterization for HO_2," *Journal of Chemical Physics*, Vol. 101, No. 5, 1994, pp. 3671-3678.

[21] Zhu, W., Wang, D. Y., and Zhang, J. Z. H., "Quantum Dynamics of Li+HF Reaction," *Theoretical Chemistry Accounts*, Vol. 96, No. 1, 1997, pp. 31-38.

[22] Fleck, Jr., J. A., Morris, J. R., and Feit, M. D., "Time-Dependent Propagation of High Energy Laser Beams through the Atmosphere," *Applied Physics*, Vol. 10, No. 2, 1976, pp. 129-160.

[23] Zhang, D. H., and Zhang, J. Z. H., "Full-Dimensional Time-Dependent Treatment for Diatom-Diatom Reactions: the H_2+OH Reaction," *Journal of Chemical Physics*, Vol. 101, No. 2, 1994, pp. 1146-1156.